Speed of sound measurements in liquid methane (CH4) at cryogenic temperatures between (130 and 162) K and at pressures up to 10 MPa

Speed of sound measurements in liquid methane (CH_4) at cryogenic temperatures between (130 and 162) K and at pressures up to 10 MPa

G. Cavuoto[a], S. Lago[a], P. A. Giuliano Albo[a], D. Serazio[a]

[a]*Istituto Nazionale di Ricerca Metrologica (INRiM), Strada delle Cacce 91, 10135 Torino, Italy*

Abstract

This paper reports speed of sound experimental measurements in liquid methane (CH_4) along five isotherms, in the temperature range of (130 and 162) K, and for pressures up to 10 MPa. A dedicated experimental apparatus, custom-designed for accurate speed of sound measurement at cryogenic temperatures and high pressures, has been developed and the *double pulse-echo* technique has been adopted. In order to characterize this new apparatus and its performance, experimental results have been compared with speed of sound values of liquid methane available in literature. A further comparison has been made between the experimental measurements and the speed of sound values obtained using the reference equation of state of methane of Setzmann and Wagner, as well as the GERG-2008 model. The ultrasonic path-length has been calibrated using pure water as a reference fluid, with a relative uncertainty of 0.026 %. The temperature was measured with two platinum resistance thermometers with an absolute uncertainty of 0.02 K. Thermometers have been calibrated using the ITS-90 temperature scale between the triple point of argon and the triple point of water. Finally, the relative expanded uncertainty (k=2) associated to the obtained results is of 0.4 %, mainly influenced by the repeatability of the measurements.

Keywords: Speed of sound, methane, lng, natural gas, cryogenic conditions

Email address: g.cavuoto@inrim.it (G. Cavuoto)

1. Introduction

Demand for an even more accurate thermodynamic properties of pure methane is showing a significant increase since liquid methane can be used as fluid and it is one of the most promising candidates for storing and trading energy. Nowadays, natural gas, in which methane is the main component, is becoming increasingly important because of its rising relevance as energy source. Indeed, its request for industrial purposes and technological processes is growing by almost 2 % per year [1], making it the fastest growing fossil fuel market today. Furthermore, it is considered a clean energy source because the products derived from its combustion, such as fine dusts and nitrogen oxides, are significantly reduced if compared with those of oil and coal. In general, its carbon footprint is smaller than that of other fossil fuels. Moreover, Liquefied Natural Gas (LNG) has shown to be particular suitable for storage, handling and transportation between tanks and tankers, tankers and ships and, in general, between operators involved in the custody transfer process, for example it is odourless, colourless, not corrosive nor toxic. In addition, the ratio between the volume of a certain mass of natural gas in its gaseous phase and the volume of the corresponding mass of LNG is about 600, thereby it is possible to store and carry a considerable amount of liquefied natural gas in relatively small volumes. Broadening the knowledge of thermodynamic properties of methane and LNG has also implications from a scientific point of view. Especially, accurate speed of sound measurements can be useful to derive other thermodynamic properties, when direct determinations are difficult. In particular, speed of sound measurements have proved to be necessary in order to implement accurate fundamental equations of state (EoS) suitable to predict the thermodynamic behaviour of the fluid, both in its gas and liquid phase, thus covering a wide range of temperature and pressure. In this context, having an additional data set of speed of sound of methane at cryogenic temperatures can help to improve the mathematical and technological tools needed to monitor the thermodynamic properties of LNG during custody transfer. When possible, the comparison of the obtained results with those already available showed that the adopted equations of state can be significantly improved, particularly for terms involving caloric properties, like speed of sound and heat capacities.

Being methane the principal constituent of LNGs, and improved formulation for pure methane lead to more reliable predictions of mixture properties.

Currently, there are some experimental works concerning speed of sound measurements of methane in literature. Unfortunately, only a few of them investigated the liquid phase due to the great complexity required to realize experimental devices capable of operating, with an acceptable accuracy, at cryogenic temperatures. First attempts to measure speed of sound of methane in gas phase was carried out by Dixton *et al*., in 1921 [2], while the first investigations into liquid methane was made in the late 1940s. In 1949, A. Van Itterbeek and L. Verhaegen [3] measured the speed of sound by acoustic interferometry methods for pressures slightly above the saturation line and for temperatures between (90 and 112) K. Although this work was the first that successfully attempted to measure the speed of sound of methane in liquid phase, results were not enought reliable, since the declared uncertainty was estimated to be up to 1 %.

A further experiment was performed by Van Dael *et al*.[4], in 1965. This was the first experimental work in which an ultrasonic *pulse-echo* technique was used at cryogenic temperature. In fact, with pulse superposition methods, speed of sound on the saturated liquid and vapour line, for temperatures between (94 and 190) K and pressures up to 4.6 MPa, were measured with a declared uncertainty of 0.1 %.

In 1967 Balgoi [5] and Van Itterbeek *et al*. [6] carried out two separate experiments designed for accurate speed of sound measurement at low temperatures. The first one used an acoustic interferometer with an uncertainty associated to the experimental results ranging from (0.3 to 1) %, while the second one used a *pulse superposition* technique claiming an overall uncertainty of 0.1 %.

In 1969, Singer [7] used a *variable-path-length* acoustic interferometer in the temperature range from (94 to 145) K and pressures from (0.2 to 9) MPa estimating an uncertainty of 0.5 %. During the mid-1970s two different works were published by Straty. In the first experiment [8], a pulsed technique was used. These measurements were made for saturated liquid methane from its triple point temperature up to 186 K, while for compressed fluid, measurements were

performed for temperatures between (100 and 300) K and for pressures up to 35 MPa with a declared uncertainty of about 0.05 %. One year later Straty carried out a further study [9], this time using a *Brillouin scattering* technique. Although the accuracy of his results was worse than that achieved in the previous experiment, it is useful to mention this work because it was the first time this type of technique was used to measure the speed of sound of methane at cryogenic temperatures. In 1975, Gammon and Douslin [10] performed measurements close to the phase boundary reaching a combined uncertainty of about 0.01 %, which nowadays is the best accuracy ever obtained for this type of measurements. For this reason the highest number of speed of sound data points selected for the formulation of the Setzmann and Wagner equation of state of methane belongs specifically to this work. Finally, it is worth mentioning the outcome Baidakov achieved in 1982 [11]. In his paper, he published results for ultrasonic speed of liquid methane in the temperature range from (150 to 183) K and for pressures up to 4 MPa. Notably, this work reports values for metastable methane for the first time. In order to obtain these results, Baidakov used a pulse technique, which is the most suitable method to carry out measurements in fluids metastable phases, since it avoid to significantly perturbe the system. The declared uncertainty of speed of sound, ignoring any side errors which could occur accross the saturation line, was 0.1 %.

Table 1 summarises the experimental techniques used in the respective works, the involved temperature and pressure ranges, as well as the uncertainties declared by authors. Finally, Figure 1 shows all (T,p) points where measurements of speed of sound were obtained. Of these, only four papers [6, 7, 8, 11] investigated the temperature and pressure ranges covered in this work. In particular, there are currently no available data for the speed of the sound of methane at T=130 K and at high pressures, so those reported in this article are the first obtained in these specific thermodynamic conditions. Finally, considering that for almost forty years no other speed of sound measurements in liquid methane have been published, the results obtained in this work will aim to enrich the state of the available data which, at the time of writing this article, is far from being complete and exhaustive.

Therefore, the experimental results obtained from the above mentioned

Authors	Technique	T / K	p / MPa	Declared uncertainty / %
Van Itterbeek *et al*. (1949)	Acoustic interferometer	90 - 112	<0.1	(2 - 5)
Van Deal *et al*. (1965)	Pulse superposition technique	94 - 190	<4.6	0.1
Balgoi (1967)	Acoustic interferometer	91 - 178	<3.2	(0.3 - 1)
Van Itterbeek, Thoen (1967)	Pulse superposition technique	111- 190	0.1-18	0.1
Singer (1969)	double pulse-echo	94 - 145	0.2 - 9	0.5
Straty (1974)	Pulsed technique	91 - 300	1.6 - 35	(0.05 - 0.2)
Straty (1975)	Brillouin scattering technique	112 - 300	<17.6	0.5
Gammon *et al*. (1975)	Acoustic interferometer	113 - 323	0.1 - 24	(0.01 - 1)
Baidakov *et al*. (1982)	Pulsed technique	150 - 183	<4	0.1

Table 1: List of speed of sound experimental data of methane at cryogenic temperature.

works were used as guide line to validate the speed of sound measurements obtained with the new apparatus presented in this work. In addition, a further comparison has been made between the experimental measurements and the expected values. These reference values have been obtained by using two different mathematical models: the reference equation of state of methane of Setzmann and Wagner [12] and the GERG-2008 model [13], which is the ISO Standard (ISO 20765-2) for the calculation of thermodynamic properties of natural gases and similar mixtures. Another model, called EOS-LNG [14], was published in 2019 for the calculation of the thermodynamic properties of LNG. This model is an enhancment of GERG-2008 and brings significant improve-

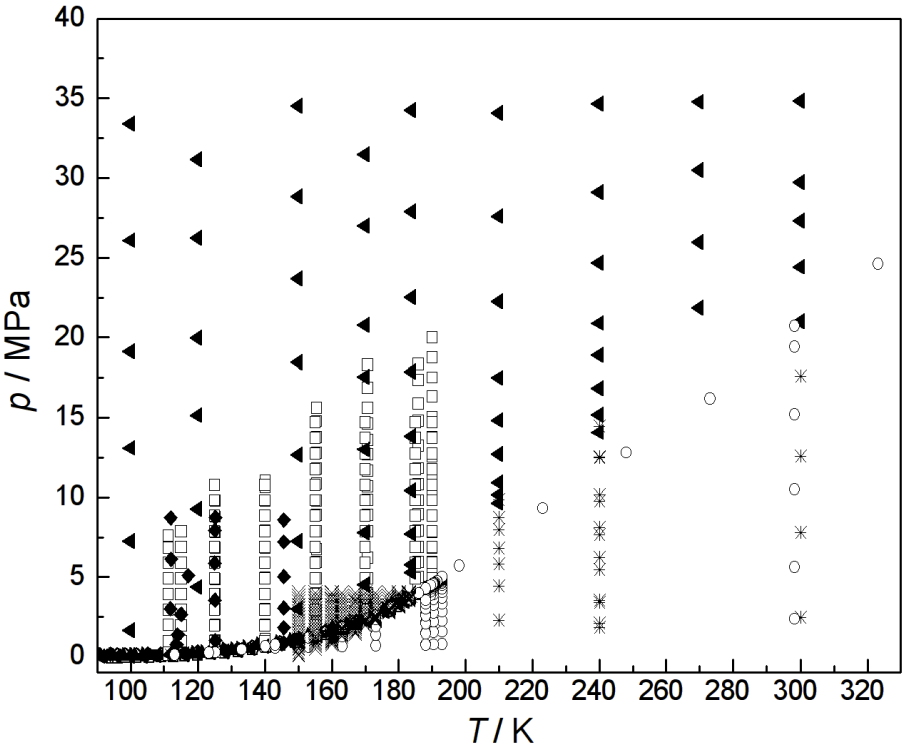

Figure 1: $T - p$ Conditions where speed of sound experimental results of liquid methane are available on literature. (■) Van Itterbeek (1949) ; (□) Van Itterbeek (1967); (⬠) Van Dael (1965); (▲) Balgoi (1967); (◆) Singer (1969); (◄) Straty (1974); (∗) Straty (1975); (○) Gammon (1975); (×) Baidakov (1982)

ments, mainly due to the inclusion of experimental density measurements between (100 and 180) K and pressures up to 10 MPa and because of the use of new binary-specific functions for mixtures of methane + n-butane, methane + isobutane, methane + n-pentane, and methane + isopentane. Despite these improvements, EOS-LNG is a model that focuses mainly on the calculation of the thermodynamic properties of LNG mixtures. For pure fluids, such as methane, the results provided by this model are the same as those obtained using GERG-2008. For this reason, it was decided to use only GERG-2008 for comparisons with experimental results while the EOS-LNG model will certainly be added to

the comparisons with speed of sound measurements of LNG mixtures, which will be carried out in the near future as the next step of this research.
The equation of state of methane of Setzmann and Wagner gives an uncertainty for the speed of sound which ranges from (0.15 to 0.3) %, for the region of pressures and temperatures of interest in this work. On the other hand, GERG-2008 model declares an uncertainty which ranges from (0.5 to 1) %, within the same $T - p$ region.

2. Experimental

2.1. Measurement technique

The measurement method is based on the *double pulse-echo* technique, which is a well known and established method, widely used for speed of sound measurements in fluids [15, 16, 17]. Besides the advantages provided by this experimental technique, it is also important to underline its suitability for the development of sensors which can be used for *on-line* measurements allowing, for example, the possibility of calibrating ultrasonic flow meters, directly in the vicinity of extraction sites or transport facilities, such as pipelines and LNG carriers. This technique make use of a piezoelectric ultrasonic transducer, working both as an emitter and receiver, excited at its resonance frequency when immersed in the fluid sample. A function generator excites the piezoceramic transducer with a sinusoidal tone-burst. After being vibrated, it yields an acoustic wave that spreads simultaneously in opposite directions following two acoustic paths L_1 and L_2 of different lengths. Each acoustic wave burst is reflected to the transducer. The electrical signal sent by the function generator to the transducer as well as the echoes from the reflectors are sampled by a digital oscilloscope. The digital signal $P_1(t_i)$, corresponding to the first echo, is correlated to the second echo $P_2(t_j)$, coming from the farthest reflector, by a temporal correlation function $C(\tau)$.

$$C(\tau) = \int_{-\infty}^{+\infty} P_1(t)P_2(t+\tau)dt, \tag{1}$$

where each $\tau \in [-\infty, \infty]$ represents the time shift between the two echoes $P_1(t_i)$ and $P_2(t_j)$. Then, evaluating the value τ_{exp} that maximizes the function $C(\tau)$, it is possible to determine the time-delay between two consecutive echoes. An easy and useful mathemderivedatical method to calculate this value is based on the *Fast Fourier Trasform* (FFT) algorithm. Indeed, starting from the properties of Fourier transforms it is possible to state that

$$\mathcal{F}(C) = \mathcal{F}(P_1)^*\mathcal{F}(P_2), \tag{2}$$

where operator $\mathcal{F}$ represents the Fourier transform (numerically implemented by FFT) of the signals. This expression leads to the possibility of obtaining the correlation function $C(\tau)$ as the inverse transform of $\mathcal{F}(C)$.

The experimental speed of sound w_{exp} is then calculated as the ratio between the space $2\Delta L = 2(L_2 - L_1)$ and the time of flight τ_{exp}, between the two echoes.

$$w_{exp} = \frac{2\Delta L}{\tau_{exp}}. \tag{3}$$

The accuracy of this experimental measurement still suffers from some side effects which need to be taken into account in order to make the results sufficiently precise. As a matter of fact, a correction factor has to be added to both the experimental time of flight and the difference between the lengths of the ultrasonic cell. In particular the experimental time difference, τ, needs two types of corrections, namely by the effect of small thermal gradients that occur inside the cell and diffraction effects, caused by the finite dimensions of the acoustic source, in order to match the ideal condition of perfect plane waves travelling in free-space. The following time of flight correction formula has been introduced here for the first time to obtain the time-delay τ_g, which occurs in the presence of thermal gradients:

$$\tau_g = \tau_{exp}\left(1 + \frac{w_z}{\tau_{exp} w_{exp}^2}(L_2^2 - L_1^2)\right). \tag{4}$$

This correction is valid under the assumption of $w_z << w_{exp}$, where w_z is a term that represents the variation of w with respect to the length z along which the thermal gradient is measured and that can be expressed as:

$$w_z = \frac{\partial w}{\partial z} = \frac{\partial w}{\partial T}\frac{\partial T}{\partial z}. \tag{5}$$

For the specific temperatures involved in this experiment, the term $\partial w/\partial T$ is about -10.8 m $s^{-1}K^{-1}$. This term has been obtained using experimental data, as the mean dependency of w versus T of the SoS values, obtained at the same

pressures on each isotherm. Instead, the term $\partial T/\partial z$ is determined experimentally for each measurement. For comparison, a gradient of 300 mK would generate correction in the order of 0.1 % on the time of flight. However, typical gradients during the experiment were kept below 80 mK.

On the other side, the diffraction corrections can be calculated using the following expression:

$$\delta t = \frac{\phi(2L_2) - \phi(2L_1)}{\omega_0}, \tag{6}$$

where ω_0 is the pulsation of the carrier wave and $\phi(L)$ is the phase shift related to a plane wave travelling the same distance of the actual wave fronts produced by the transducer.

Once the experimental speed of sound, w_{exp}, is preliminary evaluated, the phase shift, $\phi(L)$, can be calculated as a function of both the dimensions of the cell (L_1 and L_2) and the radius b of the acoustic transducer. When this last is much smaller than the dimensions of the cell [17, 18], the following closed form can be used to determine the phase shift which occurs when an acoustic wave travels the distance L:

$$\phi(L) = \text{Arg}\left[1 - \exp\left(-\frac{iA}{2L}\right)\left(\text{J}_0\left(\frac{A}{2L}\right) + i\text{J}_1\left(\frac{A}{2L}\right)\right)\right], \tag{7}$$

where $A = 2\omega b^2/w_{\text{exp}}$, while J_0 and J_1 are Bessel functions of zero and first order, respectively.

So, finally, the corrected time-delay of our interest becomes

$$\widetilde{\tau} = \tau_{\text{g}} + \delta\tau. \tag{8}$$

A further correction needs to be applied to account for the variation of ΔL, as a function of temperature and pressure. For intermediate temperatures ($T > 233.15K$), the length variation ΔL can be calculated as

$$\Delta L(T,p) = \Delta L(T_0,p_0)\left(1 + \alpha(T - T_0) - \frac{\beta_{\text{T}}}{3}(p - p_0)\right), \tag{9}$$

Where β_T is the isotermal compressibility of the AISI-316L stainless steel and α is the thermal expansion coefficient [19]. For intermediate temperatures, the cell length changes linearly with the temperature, so the thermal expansion coefficient α is usually constant. However, this functional form cannot be used in the case of cryogenic temperatures. This assumption is no longer true for cryogenic temperatures, where this dependence is not linear anymore. Using the values available in the literature [20], $\alpha(T)$ can be calculated by a polynomial fitting function as:

$$\alpha(T) = a + bT + cT^2 + dT^3, \tag{10}$$

with $a = 5.867532 \cdot 10^{-7}$, $b = 1.405386 \cdot 10^{-7}$, $c = 5.263604 \cdot 10^{-10}$, $d = 7.604209 \cdot 10^{-7}$. In this way ΔL becomes:

$$\Delta L(T,p) = \Delta L(T_0,p_0)\left(1 + \alpha(T)\exp(\gamma) - \frac{\beta_T}{3}(p - p_0)\right), \tag{11}$$

with $\gamma = (a(T - T_0) + \frac{b}{2}(T^2 - T_0^2) + \frac{c}{3}(T^3 - T_0^3) + \frac{d}{4}(T^4 - T_0^4)$. $\Delta L(T_0, p_0)$, included in equation (11), is the difference $L_2 - L_1$, obtained by calibration with a reference fluid at ambient temperature and atmospheric pressure (T_0, p_0). This term can be calculated performing a cell calibration, using pure water as reference fluid. In fact, since its thermodynamic properties are well known over a huge range of pressures and temperatures it is possible to obtain $\Delta L(T_0, p_0)$ as

$$2\Delta L(T_0,p_0) = w_w(T_0,p_0)\tau_w, \tag{12}$$

where, w_w is the speed of sound of water and τ_w is the time-delay measured during the calibration.

Finally, the corrected speed of sound $\widetilde{w}$ of methane can be calculated as the ratio

$$\widetilde{w} = \frac{2\Delta L(T,p)}{\widetilde{\tau}}. \tag{13}$$

2.2. *Experimental apparatus*

In the present work, the speed of sound of pure liquid methane (99.9995 %, weight provided by SIAD, ITALY, see Table 2) has been obtained for temperatures between (130 and 160) K and for pressures up to 10 MPa. The apparatus is based on the *double pulse-echo* technique. Measuring the time (τ) that the emitted wave needs to travel from the acoustic source to two reflector walls and back to the transducer and knowing the difference between the two acoustic paths (ΔL), it is possible to determine the speed of sound in the sample with a considerable accuracy and resolution.

Chemical name	Source	Initial Mole Fraction Purity	Purification Method	Final Mole Fraction Purity	Analysis Method
Methane (CAS name: 74-82-8)	SIAD, ITALY	0.999995	none	-	-

Table 2: Sample table.

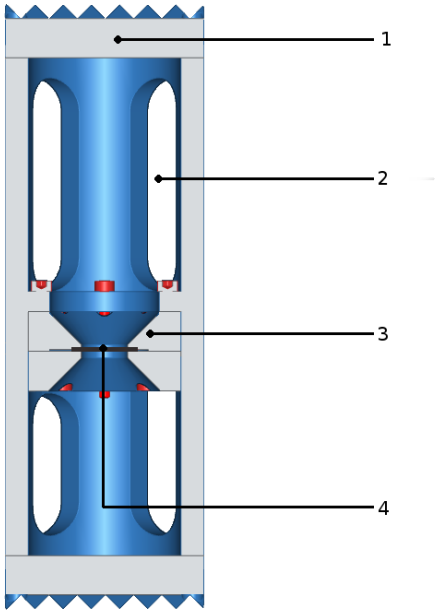

Figure 2: Front section of the ultrasonic cell. (1) Stainless steel reflector; (2) Cell eyelet; (3) Cone-shaped support; (4) Ultrasonic transducer.

Figure 3: Ultrasonic cell and vessel stopper with coupling holders.

2.2.1. The ultrasonic cell

The main component of the experimental apparatus is the ultrasonic cell, realized in stainless steel AISI 316L, with two spacers at different distances from the ultrasonic source. Figure 2 shows a longitudinal section of the measurement cell used in this work. The piezoelectric transducer (DuraAct patch, P-876K025, Piezo Technology, number 4 in the picture), has an active diameter section of 7 mm and is used both as source and receiver. Two 6 mm thick stainless steel reflectors (number 1 in the picture) are screwed to the ends of the cell. In order to minimize the effect of the back-reflections into the cell, the outer planes of reflectors were built with a series of pyramid-shaped cutting. Furthermore, the piezoelectric transducer is clamped between two cone-shaped supports (number 3 in the picture) that are used to reflect, away from the receiver, the

components of the signal that are out of the cylinder axis. Finally, on the lateral surface of the measuring cell there are eight eyelets (number 2 in the picture) which allow the cell to be completely filled and immersed within the measuring fluid.

The measuring cell is placed in a stainless steel pressure vessel capable of operating at up to 70 MPa. The inserting of the cell inside the pressure vessel, as well as its stability during the assembly of the entire apparatus and during the measurement operations, are provided by two steel coupling holders fixed to one of the vessel stopper, as shown in Figure 3.

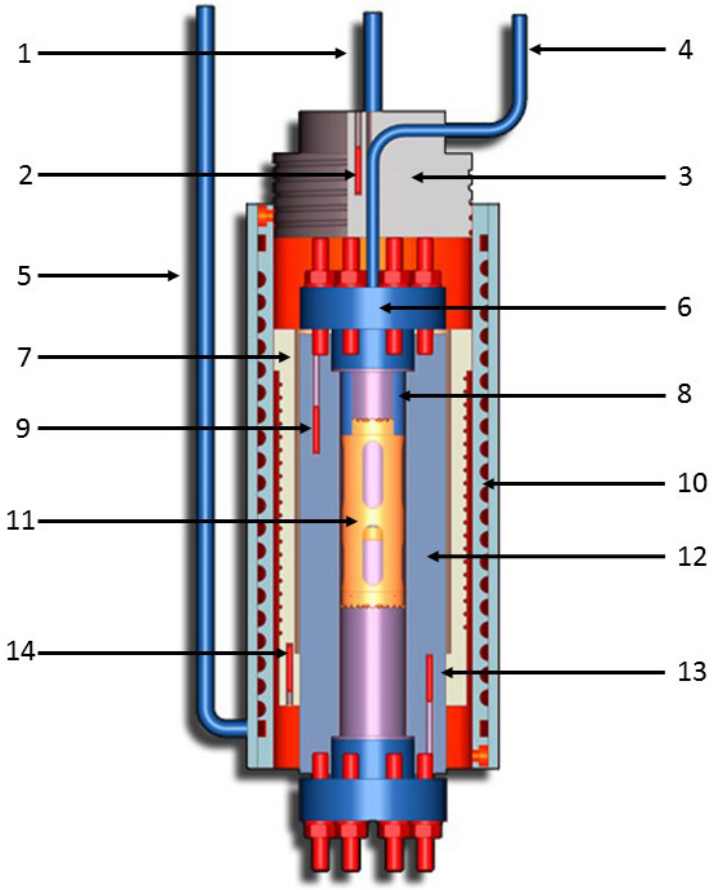

Figure 4: Cryogenic thermal apparatus:(1) LN_2 inlet; (2) Aluminium bridge thermometer, PT100; (3) Aluminium bridge; (4) CH_4 inlet; (5) LN_2 outlet; (6) Vessel stopper; (7) Thermal shield; (8) Coupling holders; (9) Upper thermometer, PT100; (10) Heat exchanger; (11) Measuring cell; (12) Pressure vessel; (13) Lower thermometer, PT100; (14) Thermal shield thermometer, PT100.

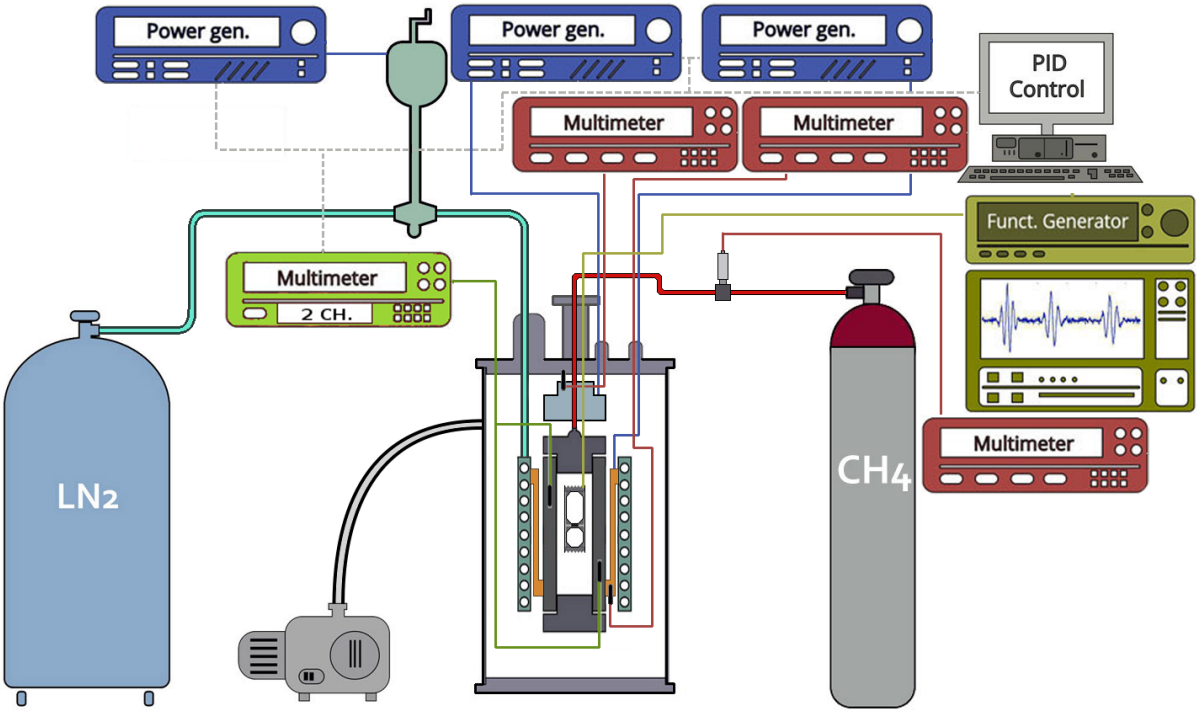

Figure 5: Cryogenic apparatus for measurements of speed of sound.

2.2.2. *Thermostatting system*

The core of the thermal unit is a thermal shield,wich is made of copper, is used to control the heat flux between an heat exchanger, where liquid nitrogen circulates, and a pressure vessel containing the liquid methane. Figure 4 reports a scheme of the thermostatting system. The thermal shield (number 7 in the picture), which can be thermally controlled, is in thermal contact with the bottom of the pressure vessel and the upper part of the aluminium cylindrical heat exchanger (number 10 in the picture). A manganin heating wire is coiled around the thermal shield in order to counteract the sudden freezing of the vessel and to stabilize the temperature at the necessary values. The thermal shield is designed with a shape that ensures, when in thermal equilibrium, a temperature stability better than 50 mK and a thermal gradient between the upper and lower part of the vessel better than 80 mK.

A platinum resistance thermometer, PT100, in thermal contact with the baseplate of the thermal shield, provides the temperature of that part of the shield that is the only section of the shield in contact with the pressure vessel. Moreover, other two platinum resistance thermometers are placed in the upper and lower part of the vessel to provide an accurate temperature measurement of liquid methane.

Despite the fact that the whole system is placed in a vacuum chamber, the inner part of the vessel is not completely thermally insulated from the outside. In fact, to inject methane into the vessel, a high pressure 1/4" inlet tube, which is directly in contact with the laboratory temperature, is connected to the upper stopper of the vessel. This configuration can generate a temperature gradient between the upper and lower edges of the vessel that can easily values above 5 K, at cryogenic temperatures. To eliminate this gradient, a further thermal bridge is used to cool down the upper part of the system. This component is a 6 cm high aluminium cylinder that is mounted to cool the inlet tube through which the methane flows. A manganin heating wire wrapped around the bridge is used to control its temperature which is measured with a PT100 thermometer placed near the methane inlet tube. Finally, to further reduce the vertical thermal gradient that may occur in the system, two additional heating wires are mounted around the stoppers of the pressure vessel. These heaters can be activated separately and they operate as thermal balancers slightly heating the part of the vessel that is colder.

2.3. Measurement procedure

Temperature of the aluminium thermal bridge as well as that of the thermal shield are measured by readings of the resistance values of two PT100, provided by two multimeters (Keithley 2000). Temperature of measuring cell is obtained as the mean value of the resistances measured by two PT100 placed inside the walls of the pressure vessel. A two-channel 8.5 digits multimeter is used to read the resistance values of both these PT100. The manganin heating wires acting on the aluminium bridge and on the thermal shield are activated by two power supplies, while the two thermal balancers are controlled by a two-output power supply. Cooling of the system is provided by liquid nitro-

gen contained in a 120 L dewar. An electro-controlled valve (Auma, Industry & Marine GmbH) is mounted between the dewar and the thermostat system. This valve is specifically designed to operate at cryogenic temperatures and it is used to adjusts the flow of liquid nitrogen inside the heat exchanger. Figure 5 shows a schematic diagram of the entire setup of the apparatus.

Considering that the cooling time-constant of the system is in the order of 8÷10 hours and the time required to take a measurement along an entire isotherm needs further 8 hours, the cryogenic valve is also used to save liquid nitrogen so that it does not run out throughout the measurement cycle. Therefore, during the cooling process from room temperature down to cryogenic temperatures, the valve is opened or closed by means of a remote control, so that the liquid nitrogen flows into the heat exchanger for 30 minutes every one hour and a half. Instead, during the measurement cycles, the valve is left open with the minimum opening to ensure the system to cool down at a rate of less than 1 K/h. Measurements are carried out for each isotherm, starting from the highest to the lowest pressure, gradually venting the methane from the pressure vessel to the atmosphere. Since, for safety reasons, it is not possible to stock liquid methane inside the pressure vessel between the isotherms, the system must be evacuated at the end of each measurement cycle, increasing the fluid temperature and opening a vent line to the outside. The whole system is isolated from the environment and placed in a vacuum chamber that is evacuated at a pressure of about $5{\cdot}10^{-3}$ mbar.

A function generator (Agilent 33250A) excites the piezoceramic disk at its resonance frequency with a periodic pulsed electrical signal. The electrical signals have a shape of five cycle pulses with a carrier frequency of 4 MHz and a peak-to-peak voltage of 10 V. The echoes received by the piezoceramic disk are recorded by a digital oscilloscope (LeCroy Waverunner 62xi) at the rate of 5 gigasample per seconds.

3. Calibration

For the temperature measurements, platinum thermo-resistances PT100 have been used. These thermometers have been calibrated at INRiM, following the same international protocol adopted for the ITS-90 calibration [24] of

Standard Platinum Resistance Thermometers (SPRT). The calibration has been carried out at the triple point of argon, the triple point of mercury and the triple point of water. The uncertainty of the thermometers has been declared to be of ±0.02 K. The pressure measurements are obtained by a temperature controlled pressure transducer (Honeywell Super TJE), placed on the hydraulic inlet line of methane, with an accuracy of ±0.025 MPa and a working range up to 51.7 MPa (as reported in the INRiM's calibration certificate). The calibration of the acoustic path-length is obtained using pure water at ambient temperature and pressure. Measured time of flight has been converted to the equivalent acoustic path-length by means of reference values of speed of sound obtained from the IAPWS-95 formulation [25]. For low pressures and moderate temperatures, this equation has a declared uncertainty of ±0.005% [26]. Using equation 12, it is therefore possible to calculate the acoustic path and, then, the dimensions of the cell. Finally, the uncertainty is calculated as shown in equation (15), using the error propagation formula, resulting in an uncertainty in the cell calibration of 0.026 %, as shown in Table 3.

4. Uncertainty analysis

The measurement technique used in this work is based on the independent determination of both the acoustic path-length, ΔL, and the time of flight, τ, that an acoustic wave needs to cover the entire length within the measurement cell. In this way, by measuring the values of T and p associated with the experimental results, it is possible to calculate the speed of sound, $w(T, p)$. The uncertainty of the measurements has been estimated taking into account the different sources contributing to its total budget, so that the estimated relative uncertainty can be calculated by using the following equation for error propagation:

$$\frac{\sigma(w)}{w} = \sqrt{\left(\frac{\sigma(\Delta L)}{\Delta L}\right)^2 + \left(\frac{\sigma(\tau)}{\tau}\right)^2 + \left(\frac{\sigma(T)}{w}\frac{\partial w}{\partial T}\right)^2 + \left(\frac{\sigma(p)}{w}\frac{\partial w}{\partial p}\right)^2 + (R)^2}, \qquad (14)$$

where R is the repeatability.

The term $\sigma(\Delta L)|\Delta L$ is the relative uncertainty associated to the acoustic path-length determination. Since this quantity is obtained by means of a cell cali-

bration, using the same experimental technique adopted for the determination of speed of sound, taking the speed of sound in water, w_w, at ambient temperature, T_0, and atmospheric pressure, p_0, as the reference value, its uncertainty is calculated in a similar way as for the uncertainty of speed of sound. In addition to this uncertainty budget, the sources of error related to the coefficient of thermal expansion, α, and the isothermal compressibility, β, which appear in equation (11), should be added. However, since these terms weight for less than 1 ppm, they have been considered negligible.

$$\frac{\sigma(\Delta L)}{\Delta L} = \sqrt{\left(\frac{\sigma(w_w)}{w_w}\right)^2 + \left(\frac{\sigma(\tau)}{\tau}\right)^2 + \left(\frac{\sigma(T_0)}{w_w}\frac{\partial w_w}{\partial T_0}\right)^2 + \left(\frac{\sigma(p_0)}{w_w}\frac{\partial w_w}{\partial p_0}\right)^2}. \qquad (15)$$

The uncertainty associated with time of flight $\sigma(\tau)$ is taken to be twice the oscilloscope sampling interval, namely $0.4 \cdot 10^{-9}$ s. Also in this case, it has been chosen to exclude from the uncertainty budget the contributions related to the time of fight corrections given by the expression (6) and (4), because they weight for less than a part per million on the uncertainty calculation.

The temperature is measured with an absolute uncertainty of 0.02 K, which is the uncertainty related to the calibration of the thermometers, while the absolute uncertainty associated with the pressure measurement is 0.025 MPa. Both temperature and pressure dependency factors, $\partial w/\partial T$ and $\partial w/\partial p$, are derived by fitting the experimental results of speed of sound. Thus, the two terms associated with the uncertainty of temperature and pressure and contained in equation (14) are uncertainty of type B. Finally, the repeatability value is estimated to be better than 0.18 %. This value has been determined after three different repeatability measurements at (134, 140 and 150) K. So, the expanded relative uncertainty in sound speed values is estimated to be 0.42 %, with a coverage factor k=2, over the entire region of measurements.

Table 3 shows the values obtained for the main uncertainty sources as well as the estimated value of the overall uncertainty of the experimental measurements of speed of sound.

Uncertainty source		Contribution / %
Acoustic path-length	$\frac{\sigma(\Delta L)}{\Delta L}$	0.026
Time of flight	$\frac{\sigma(\tau)}{\tau}$	0.004
Temperature	$\frac{\sigma(T)}{w}\frac{\partial w}{\partial T}$	0.095
Pressure	$\frac{\sigma(p)}{w}\frac{\partial w}{\partial p}$	0.072
Repeatability		0.177
Estimated expanded uncertainty (k=2)		0.42

Table 3: List of the uncertainty sources for the calculation of the overall uncertainty (with k = 2) of speed of sound.

5. Results and comments

Measurements were made along five isotherms (130, 134, 140, 150 and 162) K. For each isotherm, measurements started at the pressure of 10 MPa, down to 2 MPa. The *double pulse-echo* technique has been used.

Table 4 lists the experimental results of speed of sound in liquid methane associated with the actual temperatures and pressures of the experiment, while Figure 6 plots the adjusted values at even pressures. Any decrease in pressure, however moderate and slow over time, leads to a decrease in the methane temperature due to the adiabatic expansion inside the pressure vessel. This means that it took from 30 minutes to more than an hour, depending on the temperature at which the measurements were carried out, to restore the thermal equilibrium every time the pressure was changed. The nominal pressures taken into account for each isotherm were (10, 9, 8, 6, 4 and 2) MPa, except for the isotherm at (162, 134 and 130) K, where it has been opted to exclude the measurements at (4 and 8) MPa for T= 134 K, the points at 9 MPa for T = 130 K and at 6 MPa for T = 162 K. This decision has been taken because, during these measurements, it took longer to reach thermal equilibrium and, therefore, the consumption of liquid nitrogen to cool the system was higher, with the risk that it would run out before reaching the lowest pressures.

To verify the possibility that thermal stresses could lead to plastic deformation during the measuring cycles, the ultrasonic cell has been calibrated several times. The first calibration was performed before the measurement at (134 and 140) K, then before the measurement at 162 K, then a further calibration was

done before the isotherms at (130 and 150) K. Finally, the cell was calibrated again after the measurements were concluded. The values of $2\Delta L$ calculated after each calibration differed by about 0.01 %, showing that the cell was stable before and after each measurement.

Figure 6 shows the increasing trend of speed of sound with respect to increasing pressures, while it is clearly visible that its value increases with lower temperatures. It is also possible to see that the speed of sound is increasingly dependent on pressure, the closer it gets to the critical point.

T / K	p / MPa	w / m s^{-1}	T / K	p / MPa	w / m s^{-1}
130.03	2.13	1188.9	150.07	2.35	949.7
129.99	4.06	1212.7	150.05	4.34	988.4
129.99	6.13	1236.7	150.04	6.17	1020.3
130.06	8.05	1257.1	150.05	8.25	1053.9
130.02	10.12	1278.1	150.04	9.35	1069.7
			150.06	10.34	1082.7
133.65	2.07	1144.9	162.06	2.32	788.6
133.58	6.29	1200.3	162.07	4.16	840.2
133.68	9.22	1232.0	162.08	8.19	929.5
133.64	10.25	1243.2	162.07	9.23	949.5
			162.06	10.13	965.5
139.66	2.19	1075.3			
139.66	4.15	1104.5			
139.65	6.15	1132.5			
139.65	8.13	1158.8			
139.65	9.18	1171.4			
139.66	10.18	1184.1			

Table 4: Experimental values of speed of sound in liquid methane. Relative expanded uncertainties ($k = 2$) are $U_r(T) = 0.095$ %, $U_r(p) = 0.072$ % and $U_r(w) = 0.42$ %.

The obtained experimental values were compared with those found in literature, by interpolating the speed of sound values from the experimental data to the declared reference temperatures and pressures, by assuming a linear dependence of speed of sound for small differences of T and p. Surprisingly, the available data are quite few in the range of temperatures and pressures involved in this work. In fact, despite there are a lot of speed of sound measurements

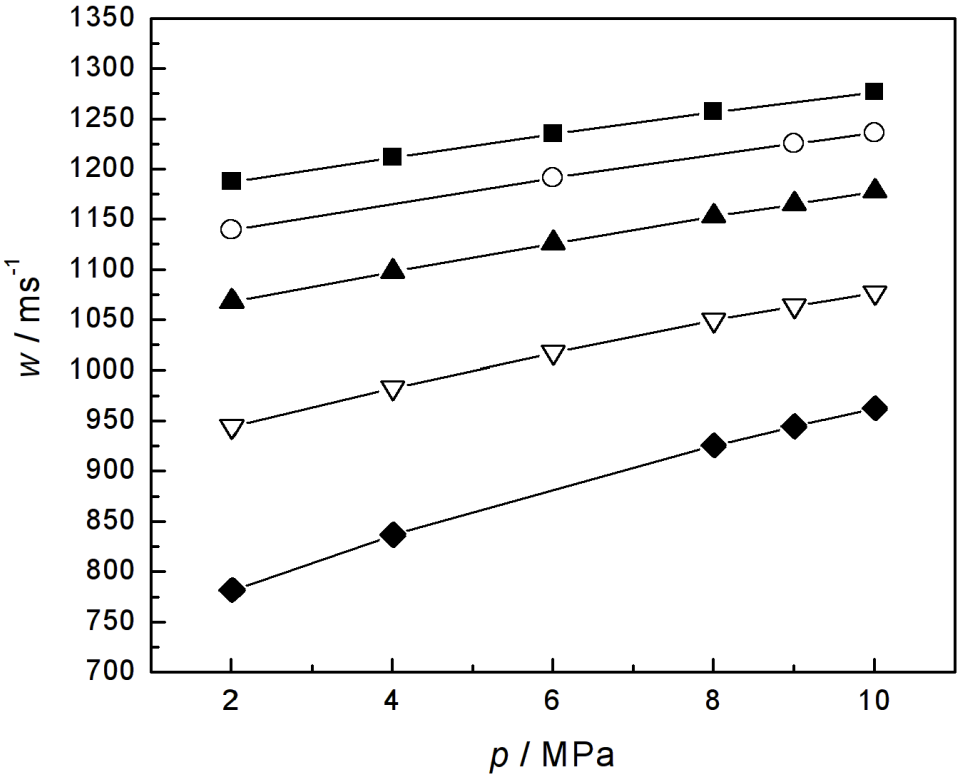

Figure 6: Experimental values of speed of sound in liquid methane along five isotherms and adjusted in order to match even values of pressure and temperature. (■) T=130 K ; (○) T=134 K ; (▲) T=140 K ; (▽) T=150 K; (◆) T=162 K .

in pure methane in the gas phase, only a few works have been carried out in liquid phase so far.

In Van Itterbeek *et al*. [6] there are 6 measurements of speed of sound at 140 K and other 6 at 155 K. Both series were carried out for pressures up to 10 MPa. Singer [7] measured 4 points at T=145.6 K for pressures up to 8.5 MPa, while only two of the measurements given in Straty [8], those at T = 150 K and pressures at (3 and 7) MPa, are within the temperature range useful for the comparison with the results of this work. Furthermore, Baidakov [11] carried out a series of measurements at pressures between (2 and 4) MPa, providing 11 values at 150 K and 15 at 160 K, where only the points corresponding to the

pressures chosen in our measurements, (2 and 4) MPa, were taken into account for the comparison. Finally, no data are currently available for speed of sound in liquid methane for temperatures between (130 and 140) K and pressures from (2 to 10) MPa.

Table 5 contains a list of all the available experimental values of speed of sound in liquid methane within the phase region under investigation. In this table their deviations from the values predicted by the reference equation of state of Setzmann and Wagner and by the GERG-2008 model are shown together with the deviations from the values obtained in this work, which are plotted also in Figure 7.

The only measurements currently available at 160 K are those of Baidakov *et al*. and deviate from the obtained measurements by less than 0.15 %, which is the uncertainty declared by the reference equation of state of methane at this temperature. Otherwise, the two points at 150 K show deviations of about 0.3 %, but they are still in agreement.

The experimental results of Singer at T=145.6 K show the highest deviations with respect to both the reference equation of state and the GERG-2008 model, especially for pressures at (3 and 5) MPa. These measurements, having a declared uncertainty of 0.5 %, have been excluded by Setzmann and Wagner's equation of state. However, by comparing them with the experimental results of this work, it can be observed the agreement is better than 0.18 %.

The two available measurements carried out by Straty at 150 K show the best agreement with the obtained measurements, deviating by less than 0.13 % at 7 MPa and by 0.03 % at 3 MPa. These data also show a very good agreement with the values obtained using the reference equation of methane, deviating from them by less than 0.02 %, while the deviations from the values obtained using the GERG-2008 model are slightly higher, but still less than 0.12 %.

Finally, the highest number of experimental speed of sound values that can be compared with our measurements is found in Van Itterbeek *et al*. For these measurements, methane with a declared purity higher than 99.95 % was used. While our experimental results are all in agreement with those of the other works found in literature, they show systematic deviations from those

Author	T / K	p / MPa	w / m s^{-1}	dev. from Setzmann & Wagner / %	dev. from GERG-2008 / %	dev. from INRIM / %
Van Itterbeek *et al.*	140.03	1.988	1059.5	0.01	-0.09	-0.79
	140.03	3.9344	1089.1	0.04	-0.08	-0.76
	140.03	5.8991	1117.9	-0.02	-0.17	-0.64
	140.03	7.8932	1145.3	-0.09	-0.25	-0.55
	140.03	8.8355	1157	-0.06	-0.23	-0.51
	140.03	9.788	1169.5	-0.12	-0.29	-0.48
	155.43	2.1451	872.9	0.23	0.30	-0.75
	155.43	3.9811	915.1	0.17	0.20	-0.55
	155.43	5.9295	954.5	0.14	0.12	-0.37
	155.43	7.8426	990.5	-0.01	-0.07	-0.16
	155.43	8.8761	1007.7	0.02	-0.07	-0.078
	155.43	9.7779	1022.5	-0.01	-0.11	0.16
Singer	145.6	8.5808	1100	-0.18	-0.03	-0.08
	145.6	7.2079	1080	-0.12	0.01	-0.18
	145.6	5.021	1050	-0.42	-0.32	0.09
	145.6	3.0597	1020	-0.66	-0.59	0.13
Straty	150	7.263	1036.6	-0.02	-0.12	-0.13
	150	3.02	962.1	-0.01	-0.03	0.03
Baidakov *et al.*	150	4.001	980.7	-0.01	-0.05	-0.27
	150	3.807	977.2	-0.02	-0.05	-
	150	3.625	973.5	0.01	-0.02	-
	150	3.419	970.0	-0.03	-0.06	-
	150	3.219	965.7	0.02	-0.01	-
	150	3.022	962.3	-0.03	-0.05	-
	150	2.825	958.1	0.01	-0.01	-
	150	2.631	954.5	-0.02	-0.03	-
	150	2.437	950.5	-0.01	-0.01	-
	150	2.242	946.3	0.02	0.01	-
	150	2.045	942.1	0.03	0.03	-0.37
	160	3.998	861.2	-0.04	0.05	0.09
	160	3.981	861.1	-0.08equation of state	0.01	-
	160	3.805	856.5	-0.04	0.05	-
	160	3.787	856.4	-0.08	0.01	-
	160	3.621	852.2	-0.08	0.02	-
	160	3.608	851.9	-0.08	0.02	-
	160	3.588	851.3	-0.07	0.03	-
	160	3.419	847.3	-0.10	0.00	-
	160	3.23	842.3	-0.09	0.02	-
	160	3.033	837.0	-0.07	0.04	-
	160	2.826	831.3	-0.05	0.07	-
	160	2.613	825.4	-0.04	0.08	-
	160	2.434	820.4	-0.04	0.09	-
	160	2.24	814.8	-0.03	0.11	-
	160	2.043	809.0	-0.01	0.13	0.13

Table 5: Available values of speed of sound in liquid methane with deviations from the predictions of the equation of state of Setzmann and Wagner and the GERG-2008 model.

of Van Itterbeek. In particular, the points at 150 K are in agreement with the reported measurements only for pressures above 6 MPa, while those at 140 K are all in disagreement with the results of this work. Since the Van Itterbeek measurements cover a wide range of pressures and temperatures and

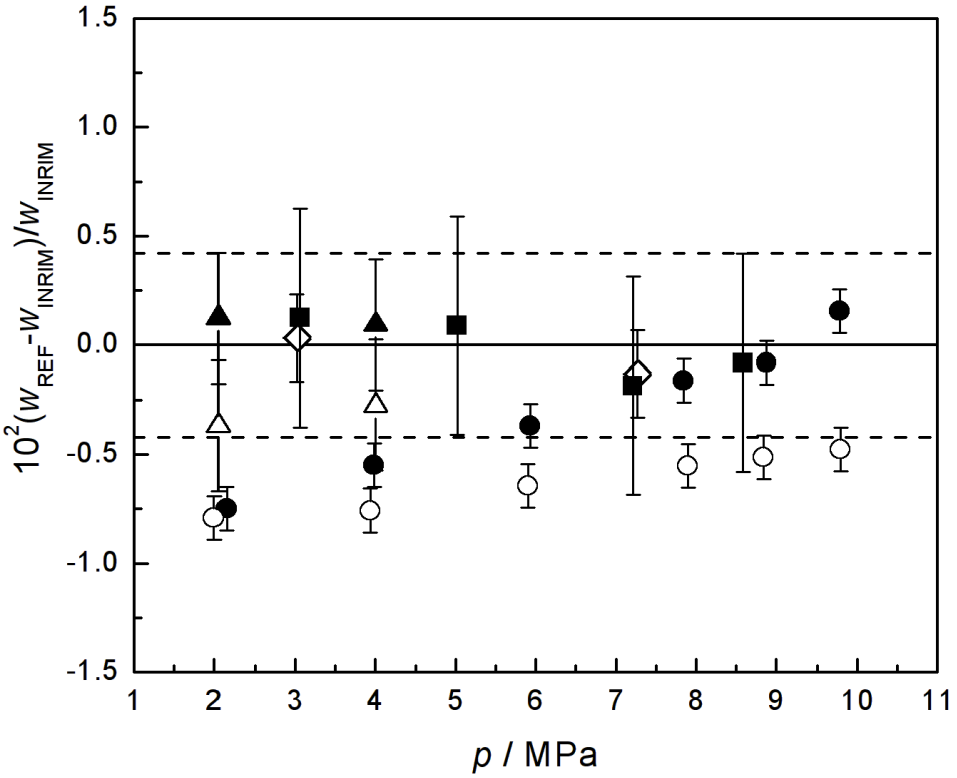

Figure 7: Deviations between the available experimental values of speed of sound in liquid methane, w_{REF}, and the new results obtained in this work, w_{INRIM}, for T=160 K and pressures between (2 and 4) MPa.(▲) Baidakov *et al*. [11] T = 160 K; (△) Baidakov *et al*. [11] T = 150 K; (●) Van Itterbeek *et al*. [6] T = 155.43 K; (○) Van Itterbeek *et al*. [6] T = 140.03 K; (◇) Straty [8] T = 150 K; (■) Singer [7] T = 145.6 K; (– –) Overall experimental uncertainty (0.42%)

also have an uncertainty of 0.1 %, which is the lowest uncertainty among the measurements obtained in this $T - p$ region, the vast majority of them have been taken as reference values for the formulation of the equation of state [12]. Nevertheless, it is important to remark that the uncertainty associated with these measurements is not explicitly indicated in the paper of Van Itterbeek *et al*. [6]. In fact, in their work, it is stated that an accuracy of 0.1 % has been obtained after the interpolation of the values from the experimental data to the pressures and temperatures tabulated by Staes [21] in his list of density data for

liquid methane. In this way, a rigorous comparison between the measurements is difficult, as the nature of the uncertainties associated with the speeds of sounds measured in this work and those associated with the Van Itterbeek measurements are substantially different.

The experimental results were then compared with the reference values predicted by the GERG-2008 model and the equation of state of Setzmann and Wagner, which is the equation used by default by the REFPROP software, developed by NIST [22]. Figure 8 shows the deviations between the experimental values of speed of sound with respect to those calculated by Setzmann and Wagner's equation, which has an estimated uncertainty for speed of sound that varies from 0.15 %, for temperatures higher than 150 K, to 0.3 % for lower temperatures. Figure 9 shows the deviations with respect to the GERG-2008 model. This model has been developed within the GERG group (Groupe Européen de Recherches Gazières) and is adopted as an ISO Standard (ISO 20765-2) for the calculation of thermodynamic properties of natural gases and similar mixtures. The state-of-the-art equation of state of methane, developed by Klimeck [23] in 2000, is used in the GERG-2008 model to calculate thermodynamic properties of pure methane. The estimated uncertainty for the speed of sound over the investigated pressures and temperatures, ranges from 0.5 %, above 150 K, to 1 % for lower temperatures.

Otherwise, for the GERG-2008 model the declared uncertainties in the investigated $T-p$ range are higher than those declared into the reference equation of Setzmann and Wagner. Comparing our results with the values predicted by both the reference equation of methane and the state-of-the-art equation of the GERG-2008 model, it is observed that deviations increase for temperatures below 140 K. To exclude potential procedural errors or poor stability conditions during the measurement cycles at these temperatures, the measurements at T = 134 K were repeated three times. Figure 10 shows the deviations of the three repetitions with respect to the mean value of the speeds of sound measured at each pressure. The repeatability of these repeated measurements is below 0.18 %.

Figure 8 shows that only the experimental results obtained at 162 K, 150 K and 140 K at higher pressures are consistent with the values predicted by the equation of Setzmann and Wagner; while, for pressures at 2 MPa and 4 MPa the experimental results are slightly outside the tolerance limit. Conversely, the measurements carried out on for isotherms at (130 and 134) K are not consistent with the values predicted by the equation. Figure 9 shows that experimental results of speed of sound are all in agreement with the values obtained from GERG-2008, except for values at 130 K and for lower pressures of the isotherm at 134 K.

The disagreement between experimental values and expected values below 140 K can be explained by analysing the lack of available data in literature for speed of sound. At present there are no experimental data at all of speed of sound in methane at 130 K and for pressures between (2 and 10) MPa. Finally,

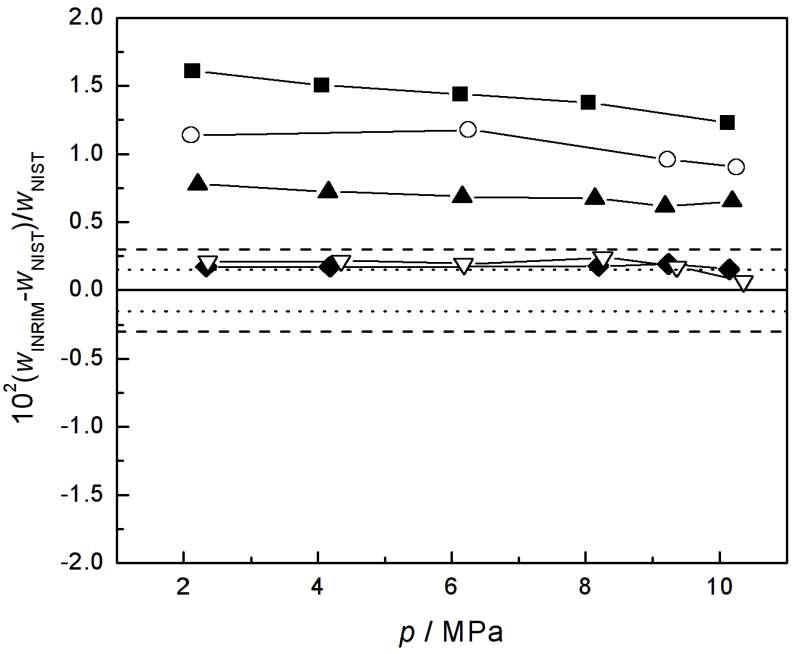

Figure 8: Deviations of experimental speed of sound of liquid methane from Setzmann and Wagner's equation. (■) T=130 K ; (○) T=134 K ; (▲) T=140 K ; (▽) T=150 K; (◆) T=162 K; (. . .) Tolerance for speed of sound above 150 K (0.15%); (– –) Tolerance for speed of sound below 150 K (0.3%).

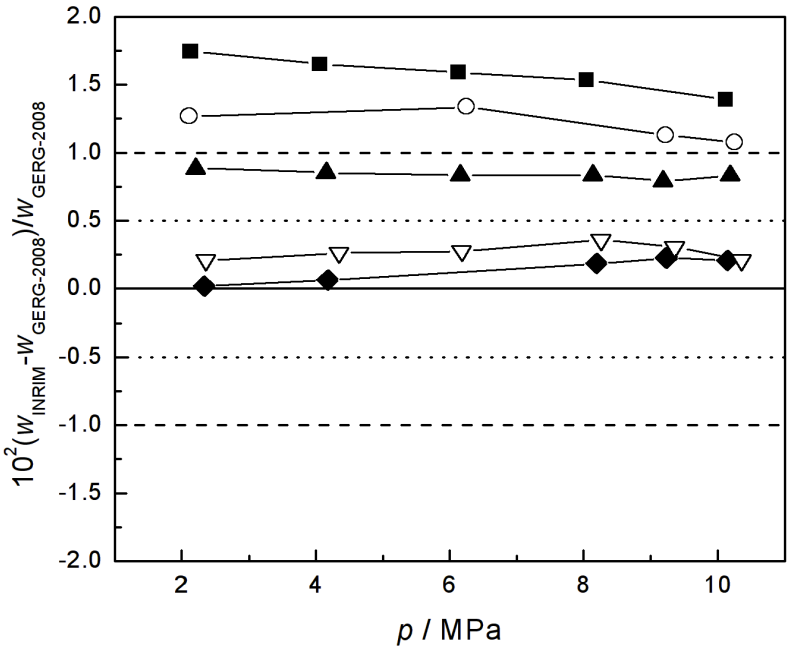

Figure 9: Deviations of experimental speed of sound of liquid methane from GERG-2008 model. (■) T=130 K ; (○) T=134 K ; (▲) T=140 K ; (▽) T=150 K; (◆) T=162 K; (. . .) Tolerance for speed of sound above 150 K (0.5%); (– –) Tolerance for speed of sound below 150 K (1%).

it should be considered that the measurements of Van Itterbeek *et al*. represent the largest number of points used for fitting the equation of state, especially for T = 140 K. Furthermore, they are the only measurements that disagree with the results here presented. It is, therefore, possible that the increasing divergences between (130 and 140) K of the experimental results here obtained with respect to those predicted by both the equation of state developed by Wagner and Setzmann and the GERG-2008 model are mainly due to the disagreement with the results of Van Itterbeek.

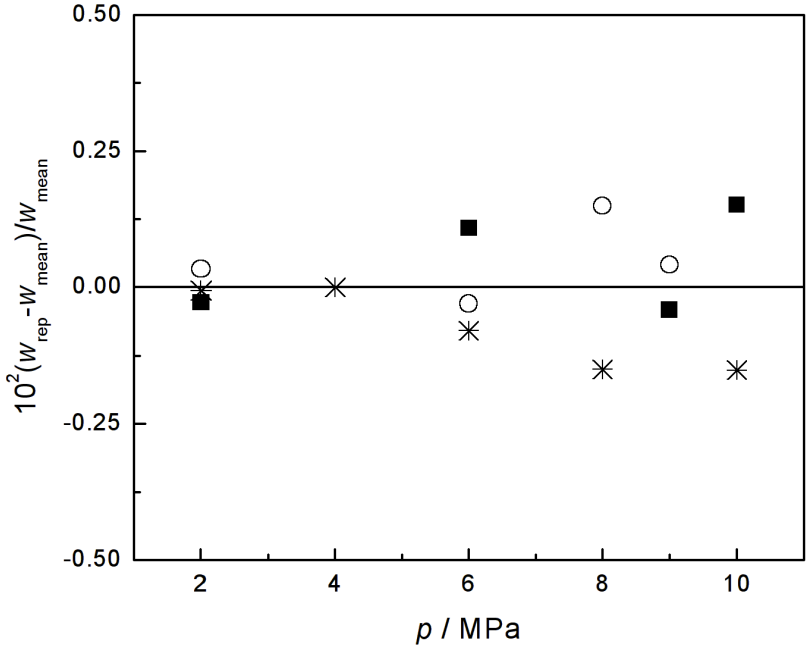

Figure 10: Deviations of speed of sound of three repeated measurements at T = 134 K from their mean value. (■) First measurement$^{(*)}$ (selected) ; (○) First repetition ; (∗) Second repetition

6. Acknowledgement

This project (16ENG09-LNG3) has received funding from the EMPIR programme co-financed by the Participating States and from the European Union's Horizon 2020 research and innovation programme.

The authors are grateful to all who have contributed to this work, especially to Marco Bertinetti for his valuable help in designing and manufacturing the copper thermal shield, the heat exchanger and the aluminium bridge used for these measurements. A special thanks also goes to Emanuele Audrito, Elio Keith Bertacco and Stefano Pavarelli for having ensured the regular supply of liquid nitrogen.

[1] GIIGNL, LNG Custody Transfer Handbook, 5th Edition (2017).

[2] H. B. Dixon , C. Campbell and A. Parker, On the velocity of Sound in Gases at High Temperatures, and the Ratio of the Specific Heats, Proc. R. Soc. Lond. 100, 1-26 (1921)

[3] A. Van Itterbeek and L. Verhaegen , Measurments of the Velocity of Sound in Liquid Argon and Liquid Methane, Proc. Phys. Soc. 62, 800 (1949)

[4] W.Van Dael, A. Van Itterbeek, J.Thoen, A.Cops, Sound Velocity Measurements in Liquid Methane, Physica 31, 1643 (1965)

[5] Yu P. Balgoi, A.E. Buko, S.A. Mikhailenko, V.V. Yakuba, Velocity of sound in liquid Kripton, Xenon, and Methane, Russ. J. Chem. 41, 908 (1967)

[6] A. Van Itterbeek, J. Thoen, A. Cops and W. Van Dael, Sound Velocity Measurements in Liquid Methane as a Function of Pressure, Physica 35, 162-166 (1967)

[7] J. R. Singer, Excess Ultrasonic Attenuation and Volume Viscosity in Liquid Methane, J. of Ch. Ph. 51, 4729 (1969)

[8] G. C. Straty, Velocity of sound in dense fluid methane, Cryogenics 14, 367 (1974)

[9] G. C. Straty, Hypersonic velocities in saturated and compressed fluid methane, Cryogenics 15, 729 (1975)

[10] B. E. Gammon and D. R. Douslin, The velocity of sound and heat capacity in methane from nearcritical to subcritical conditions and equation of state implications, J of Ch. Ph. 64, 203 (1976)

[11] V. G. Baidakov and A. m. Kaverin, Measurement of ultrasonic speed in stable and metastable liquid methane, J. of Ch. Ph. 14, 1003 (1982)

[12] U. Setzmann and W. Wagner, A New Equation of State and Tables of Thermodynamic Properties for Methane Covering the the Range from the Melting Line to 625 K at Pressures up to 1000 MPa, Journal of Physical and Chemical Reference Data 20, 1061 (1991)

[13] O. Kunz and W. Wagner, The GERG-2008 Wide-Range Equation of State for Natural Gases and Other Mixtures: An Expansion of GERG-2004, J. Chem. Eng.,57, 11, 3032-3091 (2012)

[14] M. Thol, M. Richter, E. F. May, E. W. Lemmon and R. Span, "EOS-LNG: A Fundamental Equation of State for the Calculation of Thermodynamic Properties of Liquefied Natural Gases." Journal of Physical and Chemical Reference Data 48.3, 033102 (2019)

[15] P. J. Kortbeek, M. J. P. Muringer, N. J. Trappeniers, and S. N. Biswas, Apparatus for sound velocity measurements in gases up to 10 kbar: Experimental data for argon, Review of Scientific Instruments 56, 1269 (1985)

[16] S. J. Ball, and J. P. M. Trusler, Speed of Sound of n-Hexane and n-Hexadecane at Temperatures Between 298 and 373 K and Pressures up to 100 MPa, International Journal of Thermophysics, Vol. 22, No. 2, (2001)

[17] A. Goodwin, K.N. Marsh, W.A. Wakeham, Measurement of the Thermodynamic Properties of Single Phases, IUPAC Experimental Thermodynamics Vol. VI, 435–451 (2003)

[18] P. A. Giuliano Albo, S. Lago, R. Romeo, S. Lorefice, High pressure density and speed-of-sound measurements in n-undecane and evidence of the effects of near-field diffraction. The Journal of Chemical Thermodynamics, 58, 95-100 (2013)

[19] J. R. Davis, ASM Specialty Handbook–Stainless Steels, ASM International Handbook Commiteee, (1994)

[20] R. J. Corruccini and J. J. Gniewck, Thermal expansion of technical solids at low temperatures : a compilation from the literature, National Bureau of Standards. Washington, DC, US. Gov. Printing Office 24, (1961)

[21] K. Staes, Doctoral thesis, unpublished, (1965)

[22] E. W. Lemmon, I.H. Bell, M. L. Huber and M. O. McLinden, NIST Standard Reference Database 23: Reference Fluid Thermodynamic and Transport Properties-REFPROP, National Institute of Standards and Technology, (2018)

[23] R. Klimeck, Entwicklung einer Fundamentalgleichung für Erdgase für das Gas-und Flüssigkeitsgebiet sowie das Phasengleichgewicht, Ph.D. Dissertation, Fakultat fur Maschinenbau, Ruhr-Universitat Bochum, Bochum, Germany, (2000)

[24] H. Preston-Thomas, The International Temperature Scale of 1990 (ITS90), Metrologia 27, 3 (1990)

[25] W .Wagner, A. Pruss, The IAPWS formulation 1995 for the thermodynamic properties of ordinary water substance for general and scientific use. Journal of physical and chemical reference data, 31(2), 387-535. (2002)

[26] K. I. Fuiji and R. Masui, Accurate measurements of the sound velocity in pure water by combining a coherent phase-detection technique and a variable path-length interferometer, The Journal of the Acoustical Society of America, 93(1), 276-282 (1993)